Cellulose (2023) 30:9843–9859
https://doi.org/10.1007/s10570-023-05454-8

ORIGINAL RESEARCH

Viscose nonwoven fabric with copper and its multifunctional properties

Małgorzata Cieślak · Dorota Kowalczyk · Anna Baranowska-Korczyc · Irena Kamińska · Małgorzata Krzyżowska · Martyna Janicka · Jerzy Kubacki

Received: 17 February 2023 / Accepted: 13 August 2023 / Published online: 2 September 2023

Abstract The antimicrobial functionalization of textile structures with copper and its compounds carried out by various methods increased significantly during the SARS-CoV-2 pandemic. So far, in order to obtain antiviral properties the magnetron technique using copper was applied mainly to flat textile structures; polypropylene, polyester and cotton nonwovens, and polyester and cotton woven fabrics. In this study, magnetron sputtering with copper was applied to modify the spatial viscose needle-punched nonwoven fabric. We found that the spatial nonwoven structure made of regenerated cellulose fibers and one-side sputtered with copper has strong antimicrobial activity against Gram-positive *Staphylococcus aureus* and Gram-negative *Klebsiella pneumoniae*. In the case of herpes simplex virus type 1 (HSV-1) McKrae strain, vaccinia virus (VACV) WR strain, influenza A virus H1N1 (IFV) and mouse coronavirus (MHV) JHV strain used in the study, Cu modified nonwoven fabric has only weak activity against herpes simplex virus type 1 (HSV-1). It also has no significant toxicity compared to the control medium and pristine nonwoven fabric. The modified nonwoven fabric is characterized also by hydrophobic properties, high electrical conductivity, good air and water vapor permeability, and meets the requirements of breathing resistance for all protection classes (FFP1, FFP2 and FFP3) specified in the EN 149-2001 standard.

Keywords Viscose nonwoven fabric · Copper · Magnetron sputtering · Bioactivity · Electrical conductivity · Comfort properties

M. Cieślak (✉) · D. Kowalczyk · A. Baranowska-Korczyc · I. Kamińska
Department of Chemical Textile Technologies, Lukasiewicz Research Network-Lodz Institute of Technology, Maria Sklodowska-Curie 19/27, 90-570 Lodz, Poland
e-mail: malgorzata.cieslak@lit.lukasiewicz.gov.pl

M. Krzyżowska · M. Janicka
Department of Nanobiology and Biomaterials, Military Institute of Hygiene and Epidemiology, Kozielska 4, 01-163 Warsaw, Poland

J. Kubacki
A. Chełkowski Institute of Physics, University of Silesia in Katowice, 75 Pułku Piechoty 1, 41-500 Chorzów, Poland

Introduction

Copper is one of the earliest metals known and used by man more than 10,000 years ago (Bell 2020). The first items produced were mainly ornaments, but over the years, further properties of copper and new applications were discovered. The advantages of copper were appreciated when there was no documented scientific research about microorganisms and the mechanism of their neutralization as well as advanced techniques of material modification and precise assessment of bioactivity effects (Grass et al. 2011; Borkow 2012; Hans et al. 2013). Currently, copper

has very wide areas of application, including textiles. The functionalization of textile structures with copper and its compounds is carried out by various methods to impart conductive properties (Peng et al. 2018; Nowak et al. 2019), PEM protection (Bula et al. 2006; Ziaja et al. 2008; Wiśniewski and Koprowska 2014; Koprowska et al. 2015), hydrophobicity (Peng et al. 2018), bioactivity against microorganisms (Borkow et al. 2010; Champagne et al. 2019; Kudzin et al. 2020; Marković et al. 2020; Cieślak et al. 2022; Sharma et al. 2022), and UV protection (Vihodceva et al. 2011; Peng et al. 2018; Kudzin et al. 2020). Such textile materials are not only bioactive (Kharaghani et al. 2018; Gurianov et al. 2019; Hashmi et al. 2019; Liu et al. 2021) but also multifunctional (Ali et al. 2018; Huang et al. 2022).

The interest in antiviral modifications increased significantly during the SARS-CoV-2 pandemic (Imani et al. 2020; Balasubramaniam et al. 2021; Lin et al. 2021; Hussain et al. 2022; Meister et al. 2022). One of the modification methods which enables the application of thin metallic layers on the surface of various materials is Physical Vapor Deposition (PVD) (Kelly and Arnell 2000; Vihodceva et al. 2011; Markowska-Szczupak et al. 2021). In the case of textiles, depending on their applications, it is important to select the appropriate metal and its form, as well as the type of raw material and its structure. So far, in order to obtain antiviral properties, including against SARS-CoV-2, the magnetron technique using copper was applied mainly to polypropylene spunbond nonwoven (Jung et al. 2021), polyester nonwoven (Jung et al. 2022), polyester and cotton woven fabric (Cieślak et al. 2022), and cotton nonwoven (Zhang et al. 2022). In our previous work, it was found that two flat textile structures—a polyester woven fabric with an admixture of polyamide and a cotton woven fabric, sputtered with Cu in the same way, showed different bioactive properties (Cieślak et al. 2022). Both fabrics have strong antibacterial activity against *Staphylococcus aureus* and *Klebsiella pneumonia*, but in the case of antiviral test the results were varied. Cu-cotton fabric has good antiviral activity in relation to vaccinia virus (VACV), herpes simplex virus type 1 (HSV-1) and influenza A virus H1N1 (IFV), while its antiviral activity against mouse coronavirus (MHV) is weak. Cu-polyester fabric has weak antiviral activity against HSV-1 and MHV. Since Cu modified cellulose flat woven fabric showed greater activity against viruses, we wanted to investigate whether a nonwoven fabric with a spatial 3-D structure made of regenerated cellulose fibers and modified in the same way would have similar antimicrobial properties. To the best of our knowledge, there are no publications on viscose textile structures sputtered with copper by magnetron technique to obtain antibacterial and antiviral properties. In our previous research polyester and cotton fabrics had flat structures and copper homogenously sputtered the whole fibres surface, which allows interact with the viruses efficiently and results in high antimicrobial properties.

In this study, magnetron sputtering method is applied for the first time to modify of viscose needle-punched nonwoven with copper. A significant advantage of this method is preserving the structure properties of the nonwoven fabric during modification process, but the modification effect of spatial structure with this technique may be different compared to flat structures. After the magnetron sputtering with Cu viscose needle-punched nonwoven is characterized by antimicrobial activity, hydrophobic properties and high electrical conductivity. These new features can extend the applications of viscose textile structures to design antibacterial and antiviral, and electrically conductive textile systems. Developed materials may be used in protective mask, clothing or as special packaging and coverings *inter alia* in the area/devices protected against Electrostatic Discharge (ESD).

Materials and methods

Textile structure

Viscose (VI) needle-punched nonwoven with the characteristic presented in Table 1 was used in the study.

Methods

Modification of nonwoven with copper by magnetron sputtering

Modification of nonwoven with copper was carried on the DC magnetron sputtering system, (P.P.H. Jolex s. c., Czestochowa, Poland) equipped with a pulse current source with a power of minimum 12 kW and a

Table 1 Characteristic of viscose needle-punched nonwoven

Material structure	Needle-punched nonwoven
Fibers apparent diameter*, μm	20.3 ± 1.49
Fibers lenght, mm	56.7 ± 2.30
Volume porosity**, %	96.46
Mass per unit area, g/m^2	184 ± 2
Thickness, mm	4.15 ± 0.23

*The fibers diameter was determined with scanning electron microscopy (SEM) technique

**The percentage of air in the volume of the nonwoven

maximum voltage of 1.2 kV with an adjustable group frequency from 50 to 5 kHz (Koprowska et al. 2015). The process was carried out on the nonvowen sample, in an inert gas—argon using the copper target with a purity of 99.99% (Testbourne Ltd., Basingstoke, UK) and following conditions: pressure of 2.0×10^{-3} mbar, effective power of 2.0 kWh, circulating power of 0.8 kWh, argon content of 3%, sputtering time of 10 min.

Microscopic analysis

SEM microscopic analysis were carried out on a scanning electron microscope VEGA3 (TESCAN, Czech Republic), using the high vacuum mode, secondary electron (SE) detector and the energy of probe beam of 20 keV. The samples were sputtered with gold on the Quorum Technologies Ltd. vacuum device. The elemental analysis was performed on the EDS INCA Energy spectrometer (Oxford Instruments) on the samples without sputtering with gold. X-ray microanalysis was done under air pressure of 10 Pa, using an accelerating voltage of 20 kV, backscattered electron beam (BSE) and the SmartMap function. For each sample, maps of the distribution of elements, the total spectrum as well as weight and atomic percentages of elements were prepared. The maps were determined for the elements C, O and Cu for the Kα line with the excitation energy E = 0.28 keV, E = 0.52 keV and E = 8.04 keV, respectively.

Fourier transform infrared spectroscopy (FTIR), Raman and XPS spectroscopies

The infrared spectra were recorded by a BRUKER Vertex 70 FTIR spectrometer (Bruker, Germany) using a diamond Attenuated Total Reflection (ATR) accessory. FTIR absorption spectra were measured in the wavenumber range of 600 to 4000 cm^{-1} with a resolution of 2 cm^{-1}. The Raman spectra were examined using an inVia Renishaw Raman Microscopy System (Renishaw, GB). The excitation source was a semiconductor laser with a wavelength of 785 nm. The laser beam was focused on the samples using a 50× objective lens. Each spectrum was collected with four accumulations in the wavenumber range of 200–3200 cm^{-1}.

The XPS spectra were recorded at room temperature in a PHI 5700/660 physical electronics photoelectron spectrometer (Physical Electronics, USA) using a monochromatized Al Kα ($h\nu = 1486.6$ eV) X-ray source.

Determination of Cu content

In order to determine the copper content in the nonwoven, the sample was mineralized in a microwave mineralizer (Magnum II, Ertec, Poland). Then, the mineralized sample was dispersed in purified water. The content of copper in the dispersion was determined by means of an atomic absorption spectrometer (AAS) with flame atomization (SpectrAA 250 Plus, Varian, Australia).

Thermogravimetric analysis

Thermogravimetric analysis TG/DTG was performed using thermogravimetric analyzer TG 209 F1 Libra (Netzsch, Germany) in the temperature range 30–680 °C with a heating rate 10 °C/min. Samples with a mass of 4 mg were tested in a ceramic crucible with a volume of 85 μl in a nitrogen atmosphere (gas flow of 25 mL/min.). Three repetitions were used.

The initial (TOnset), final (TEnd), and the peak maximum (TPeak1) temperature of the thermal degradation process and the weight loss of samples at 680 °C were determined.

Antibacterial test

The test was performed according to PN-EN ISO 20743:2013-10 *Determination of antimicrobial activity of finished products with antibacterial finish* using the bacteria strains of Gram-positive *Staphylococcus aureus* (ATCC 6538) and Gram-negative *Klebsiella*

pneumoniae (ATCC 4352). The pristine textile structures are used as reference materials. Assessment of antibacterial activity (A) was carried out according to EN ISO 20743:2013 Appendix F, where $2 \leq A < 3$ means significant and $A \geq 3$ strong bioactivity.

Antiviral and cytotoxicity tests

For assessment of antiviral activity four pathogens were used: herpes simplex virus type 1 (HSV-1) McKrae strain (Gothenburg University, Sweden), vaccinia virus (VACV) WR strain (ATCC VR- 1736), influenza A virus H1N1 (IFV) (ATCC VR-1736) and mouse coronavirus (MHV) JHV strain (ATCC VR-765). Tests with HSV-1 and VACV were performed in Vero cells (ATCC CCL-81) cultured in Dulbecco's Modified Eagle's (DMEM) Medium with GlutaMAX supplemented with 10% fetal bovine serum (FBS), 100 units/mL penicillin, 100 µg/mL streptomycin (Thermo Fisher Scientific, Waltham, MA, USA). Vero cells were inoculated with cryopreserved HSV-1 or VACV. The virus infection was monitored by observable cytopathic effects (CPE). The virus stock infectivity titer (plaque forming unit (PFU)/mL) was determined in Vero cells inoculated with serial dilutions of virus suspensions. After 48 h, infected cell cultures were stained with 1% crystal violet and used to determine the number of cytopathic effects per mL (PFU/mL) (Szymańska et al. 2018). Tests with IFV were performed in MDCK (NBL-2) (ATCC®, Manassas, VA, USA, CCL-34) cells cultured in DMEM medium with antibiotics and 10% FBS (Thermo Fisher Scientific). MDCK cells were inoculated with cryopreserved IFV, then cultured for 72 h and monitored for observable cytotoxic effects. Tests with MHV virus were performed in NCTC clone 1469 cells (ATCC® CCL-9.1), cultured in Minimum Essential Media (MEM) with antibiotics and 10% FBS (Thermo Fisher Scientific). The infected cultures were observed for 24 h for the presence of CPE.

For MHV and IFV, TCID50/mL (Spearman-Kärber method) (Kärber 1931) was used to determine the concentration of the inoculated virus based on the outcome of the end-point dilution resulting in the CPE of the MDCK (IFV) or NCTC (MHV) cells cultured in 96 well plates. The mouse beta-coronavirus (MHV) was chosen in context of future research concerning the SARS-CoV-2. It is an enveloped virus with a positive-sense RNA genome in the Coronaviridae family and has been studied widely as a model of viral pathogenesis (Miura et al. 2008). The study was performed according to the standard 18,184:2019 *Textiles-Determination of antiviral activity of textile*, in which good antiviral activity is described as $3.0 > Mv \geq 2.0$. As a negative untreated test control material, the pristine fabric was used. The control and modified fabric samples were cut into 1.0 g pieces, autoclaved in order to sterilize and next inoculated with 0.2 mL of the viral inoculum. Incubation was carried out at room temperature for 2 h. Each of samples was prepared in triplicates. All samples were washed with 20 mL of the neutralizing solution (complete cold medium), followed by 1 min of vortexing. Aliquots of the neutralizing solutions were used to determine the infectious titer of the recovered virus by PFU/mL (HSV-1, VACV) or TCID50/mL (IFV, MHV) method.

The antiviral activity (Mv) value was calculated according to the equation:

$$Mv = -\log(Vc/Vt) = -[\log(Vc) - \log(Vt)],$$

where log(Vc) = the common logarithm average of three infectivity titer values immediately after inoculation of the control sample; log(Vt) = the common logarithm average of three infectivity titer values immediately after the 2 h contact time with the tested samples. According to the standard 18,184:2019, good antiviral activity is described as $3.0 > Mv \geq 2.0$.

In order to assess potential cytotoxicity, the following test was conducted: 20 mL of the neutralizing solution was added to non-virus inoculated control and test samples, incubated for 2 h and after vortexing, aliquots from these solutions were added to the Vero cells. Cytotoxicity was then monitored with MTT cell viability assay according to the producer's manual (Thermo Fisher Scientific).

Determination of wettability and surface free energy

The contact angle θ was determined using a PGX goniometer (Fibro System AB, Sweden). Three wetting liquids with known values of surface free energy (γ_L) and its dispersion and polar components (γ_L^d,γ_L^p) were used: water, W ($\gamma_L = 72.80$ mJ/m^2, $\gamma_L^d = 21.80$ mJ/m^2, $\gamma_L^p = 51.00$ mJ/m^2), formamide, F ($\gamma_L = 58.00$ mJ/m^2, $\gamma_L^d = 39.00$ mJ/m^2, $\gamma_L^p = 19.00$ mJ/

m^2), hexane, H ($\gamma_L = 18.40$ mJ/m^2, $\gamma_L{}^d = 18.40$ mJ/m^2, $\gamma_L{}^p = 0$ mJ/m^2). The droplet volume was 3 µL, temperature 22.3 ± 1 °C, RH = 40 ± 1%. Three repetitions for each sample were made and mean values and standard deviation were determined. Based on the mean value of the contact angles, the surface free energy and its components were calculated according to the Owens–Wendt method (Owens and Wendt 1969; Cieślak et al. 2012).

Measurement of electrical properties

Surface (Rs) and volume (Rv) electrical resistance of nonwovens was measured according to standard PN-P-04871:1991 *Textiles. Determination of electrical resistivity,* using a set of standardized electrodes, a digital DM53 multimeter (Polmed, Poland) and 6206 teraohmmeter (ELTEX, Germany). The half decay time of electrostatic charge (t_{50}) and shielding factor (S) were determined according to standard PN-EN-1149-3:2007 *Protective clothing. Electrostatic properties. Part 3: Test methods for measurement of charge decay* (induction method).

All samples were tested triplicate in an air-conditioned HCZ 0030 L(M) chamber (Heraeus, Germany) at a temperature of 23 ± 1 °C and relative humidity (RH) of 25 ± 5% and 50 ± 5%. Before testing, samples were conditioned under the same conditions for 24 h.

Air and water vapour permeability

Air permeability was measured in accordance with the standard PN-EN ISO 9237:1998, *Textiles. Determination of permeability of fabrics to air*, using pressure difference of 100 Pa, temperature of 21 °C and RH = 64%. The tests were carried out on a sample with a surface of 20 cm^2.

Water vapour permeability (WVP) was measured in accordance with the standard PN-EN ISO 11092:2014-11, *Textiles. Physiological effects. Measurement of thermal and water-vapour resistance under steady-state conditions* (sweating guarded-hotplate test), using Thermetrics 306-240, Thermetrics, USA.

Breathing resistance measurement

To measure the inhalation and exhalation resistance of the viscose non-woven under specified condition the GT-RA03 Mask&Respirator Breating Resistance Tester (Quanzhou Gester International Co., Ltd, China) was used. The measuring range of flowmeter was 0–400 L/min, and the accuracy was 1%. The range of the micromanometer was 0–1000 Pa, and the accuracy was 1 Pa. According to EN 149:2001 + A1:2009 standard *(Respiratory protective devices—Filtering half masks to protect against particles—Requirements, testing, marking),* the inhalation test flow rate 30 L/min and 95 L/min, and exhalation test flow rate 160 L/min were used. The measurements were carried out at 23 ± 1 °C and RH = 40 ± 1%.

Results and discussion

SEM images (Fig. 1) show the surface of the pristine nonwoven fabric and the longitudinal and cross-sectional views of the fibers. Viscose fibers have an extended outer surface with longitudinal grooves. The distribution of the fibers is typical for a nonwoven fabric produced by the needle-punched technique, with a varied and disordered spatial structure and relatively large distances between the fibers. Such structure is characterized by high

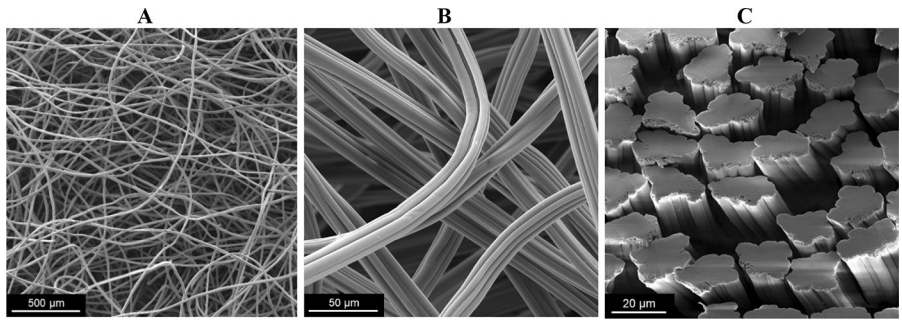

Fig. 1 The SEM images of pristine viscose nonwoven: **A** surface view, **B** longitudinal and **C** cross section of the fibers

Thickness, mm	
pristine	4.15±0.23
VI/Cu	4.17±0.11
Cu layer	1.51±0.10

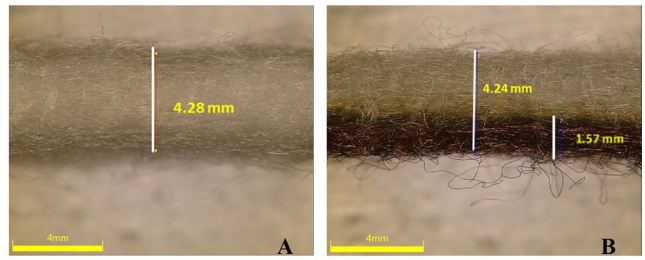

Fig. 2 The exemplary images of cross sections of **A** pristine and **B** Cu modified nonwoven with the average thickness values

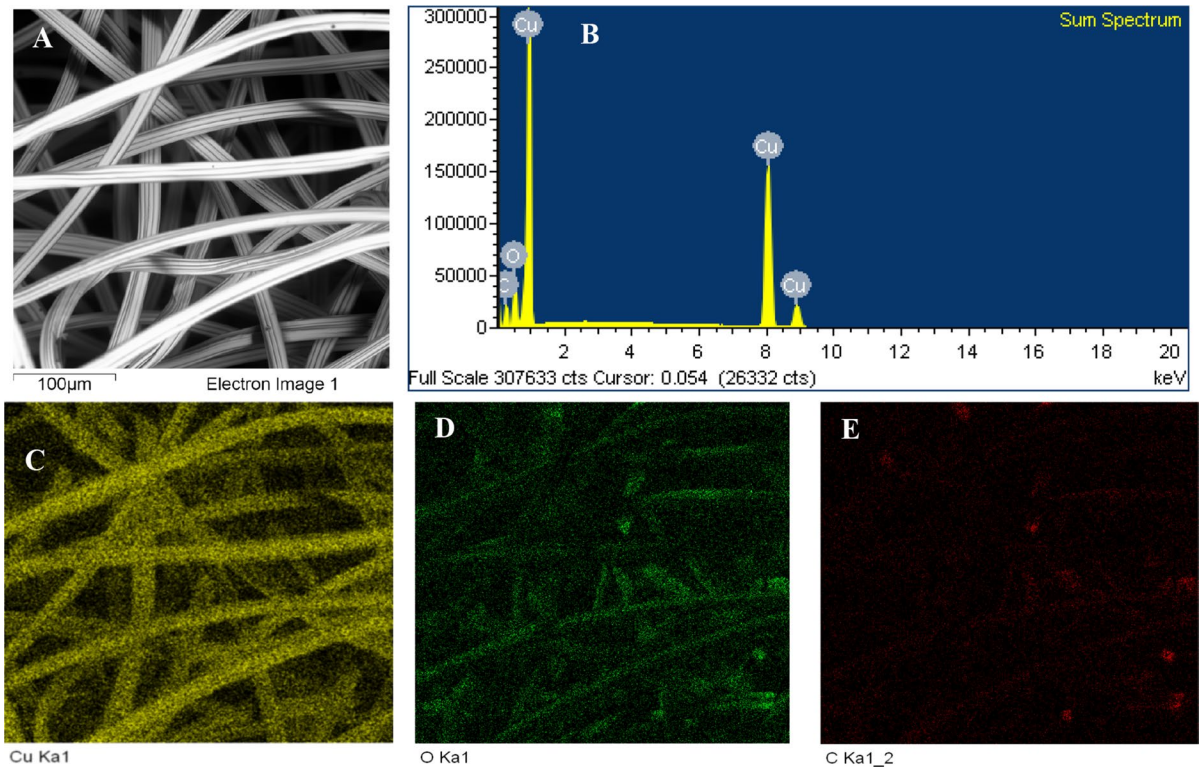

Fig. 3 Results of SEM/EDS analysis: **A** SEM images, **B** sum spectrum and **C-E** exemplary maps of elements distribution on nonwovens surface (Cu—yellow, O—green, C—red)

volume porosity of 96.46% and allows Cu particles to penetrate into the viscose nonwoven structure up to 1.51 ± 0.10 mm (Fig. 2B). The average value of thickness did not change significantly after sputtering and amounts to 4.15 ± 0.23 and 4.17 ± 0.11 mm, respectively, for pristine and Cu modified nonwoven (VI/Cu) (Fig. 2). The total Cu content determined by the AAS analysis is 22.2 g/kg (2.22%), which is 4.1 g/m^2 per unit area. SEM/EDS analysis revealed Cu content of 74.1 ± 1.43 wt% and also O and C element's presence (Fig. 3, Table 2). The SEM analysis

Table 2 Weight percentage of elements determined for pristine and modified viscose nonwoven (VI/Cu)

Elements, wt%	pristine	VI/Cu
Cu	–	74.1 ± 1.43
O	53.0 ± 0.05	10.1 ± 0.55
C	47.0 ± 0.05	15.8 ± 1.01

showed differences in the Cu coating thicknesses on the fiber surface. Some part of the viscose fibers are not covered with Cu, especially in longitudinal grooves. The varied thickness coating or its lack is the result of different position of the fibers in the spatial nonwoven fabric structure and their alignment to sputtering target (Fig. 3E, F) (Fig. 4).

Spectroscopic analysis

Since Cu is a low stable element and forms easily different oxides the spectroscopic analysis was applied to evaluate its form on viscose nonwoven fabric. FTIR spectrum of pristine nonwoven shows typical bands for viscose (Fig. 5). Main vibrational assignments

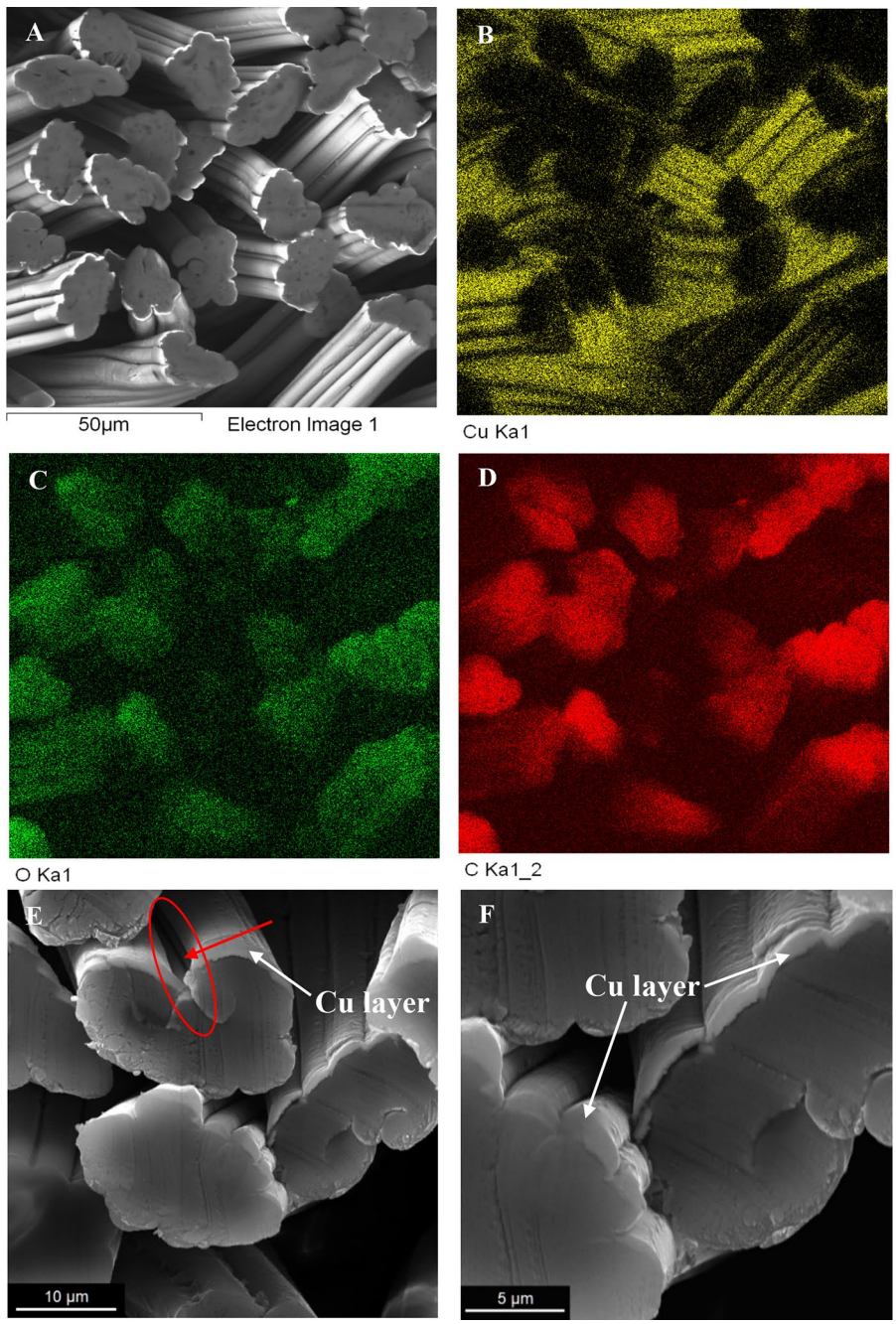

Fig. 4 Results of SEM/EDS analysis: **A** SEM images and **B-D** exemplary maps of elements distribution for fibers cross section, (Cu—yellow, O—green, C—red) and **E–F** SEM images od fibers cross section (magnification **E**—×5000, **F**—×10,000)

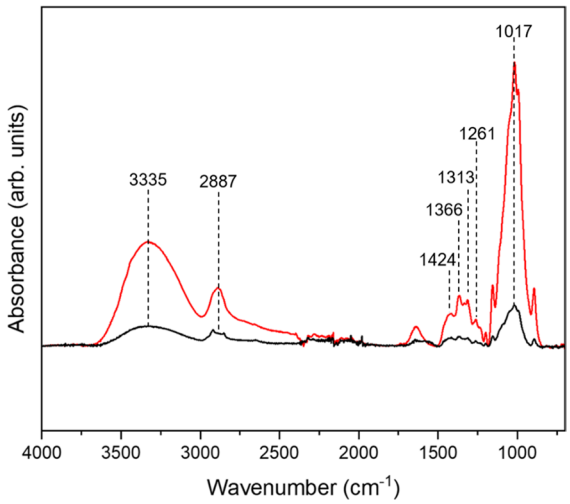

Fig. 5 FTIR spectra of pristine (red) and Cu modified (black) viscose nonwoven

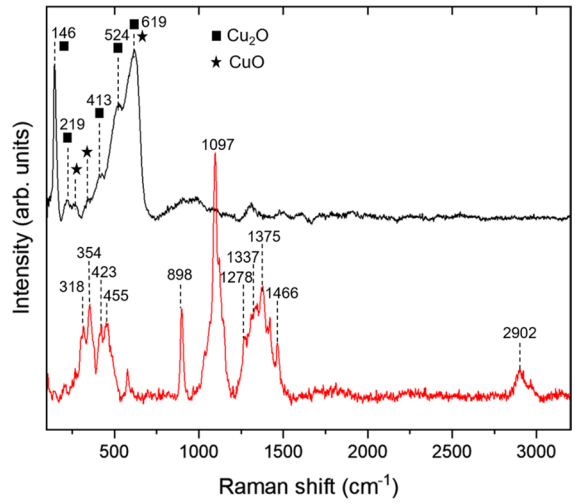

Fig. 6 Raman spectra of pristine (red) and Cu modified (black) viscose nonwoven

of viscose bands are present at 3335, 2887 and 1017 cm^{-1} and are related respectively to OH stretching, CH bending and CO stretching (Giesz et al. 2016; Sülar and Devrim 2019). Infrared bands with the maxima at 1366 and 1261 cm^{-1} correspond to CH bending, and bands centered around 1424 and 1313 cm^{-1} indicate CH_2 symmetrical bending and wagging, respectively (Carrillo et al. 2004). After modification with Cu, the intensity of the main infrared viscose bands decreased significantly confirming the formation of Cu-based compound layer on viscose.

The Raman spectra of viscose reveals clearly defined bands centered around 1096 cm^{-1} related to COC stretching (Fig. 6). The another typical band for viscose corresponded to HCC and HCO bending is noted at 898 cm^{-1} (Giesz et al. 2016). Characteristic bands centered around 1466, 1375, 1337, and 1278 cm^{-1} are related to CH_2 bending, rocking, and wagging, bands at 318, 354, 423 and 455 cm^{-1} correspond to COC and CCC bending (Was-Gubala and Machnowski 2014). The peak at 2902 cm^{-1} is related to CH stretching.

After the modification with Cu, Raman spectra shows new bands corresponding compounds based on Cu. The presence and the intensity of the bands at 146, 219, 413, 524 and 619 cm^{-1} reveal dominant contribution of Cu_2O compound (Anu and Abdul Khadar 2015; Jrajri et al. 2022). The coating is composed with copper oxides mixture due to the fact that band of low intensity of CuO are also noted at 263 and 330 cm^{-1} (Han et al. 2015). The band at 619 cm^{-1} is also partially related to the presence of CuO in the sample (Li et al. 2015).

The presence of Cu, Cu_2O and CuO was also confirmed by XPS analysis. In the XPS survey spectra of Cu modified viscose sample, the main peaks of Cu2p, O1s and C1s are observed (Fig. 7A). Deconvoluted XPS core spectrum of $Cu2p_{3/2}$ consisting of four peaks at 932.8, 935.1, 941.2 and 943.7 eV is shown in Fig. 7B. The strong peak at 932.8 eV is related to Cu or Cu_2O (Poulston et al. 1996; Biesinger 2017). Moreover, the peak at 935.1 eV accompanied with two satellites peaks at 941.2 and 943.7 eV indicates the presence of CuO in the sample (Biesinger 2017; Hiraba et al. 2021).

The broad shape of the O1s peak suggesting the coexistence of different species on the sample surface, which makes the identification of copper oxides much more difficult. Deconvoluted O1s spectrum consists of three peaks located at 530.8, 532.0 and 533.5 eV (Fig. 7C). The peak at 530.8 eV can be assumed to correspond to lattice oxygen in Cu_2O (Barreca et al. 2007; Jiang et al. 2013). The others most likely correspond to oxygen in viscose or/and originate from H_2O or OH species adsorbed on the Cu surface (Yamamoto et al. 2008). For C1s, two main peaks were detected at

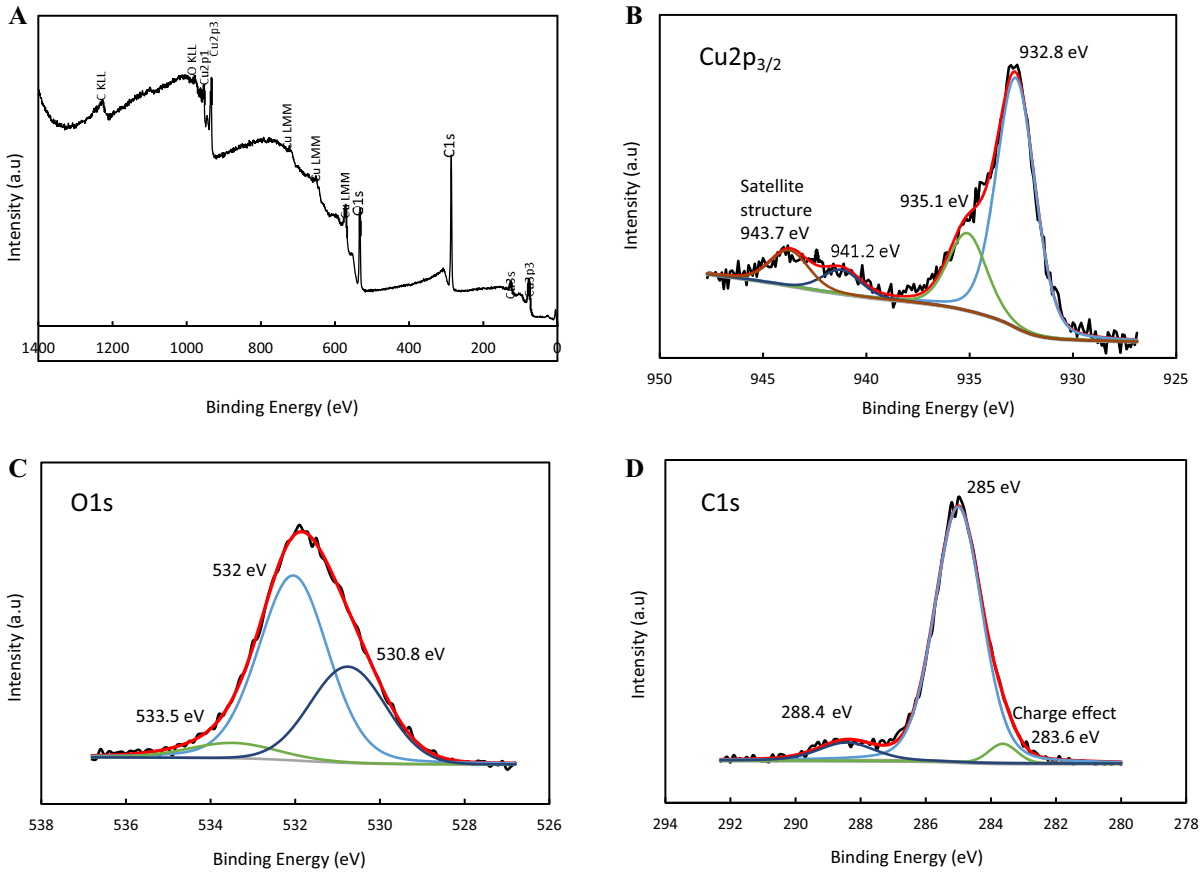

Fig. 7 **A** XPS survey spectra of Cu modified viscose and **B** high-resolution elemental spectra of Cu $2p_{3/2}$, **C** O1s and **D** C1s

285.0 and 288.4 eV which are related to carbon atom in C–C and O–C–O/C = O bonds, respectively (Fig. 7D) (Vesel et al. 2009; Dobromir et al. 2011).

TG/DTG analysis showed that a weight loss of 6.52% and 6.08%, occurs in the range of 30–100 °C, respectively for the pristine and Cu modified viscose fabric, corresponding to the water desorption process (Fig. 8). The thermal decomposition process takes place in the temperature range of 294–363 °C with a peak maximum at 341 °C. Weight loss at 600 °C is 86 ± 3%. For the Cu modified fabric, the temperature values do not change significantly. The value of weight loss decreases to 84 ± 1%, which indicates that the copper content on the modified nonwoven fabric is about 2%. Cu content evaluated by TG analysis confirms the previous results obtained from AAS.

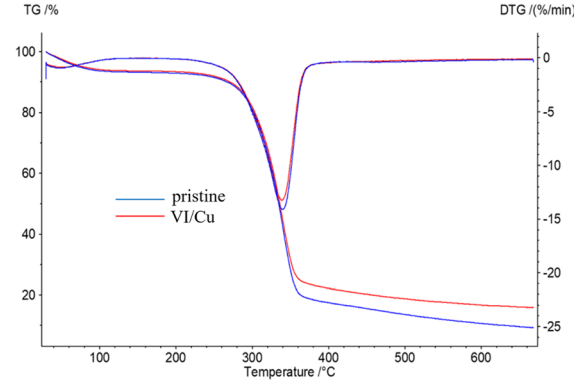

Sample	T_{Onset} [°C]	$T_{End.}$[°C]	T_{Peak} [°C]	Weight loss [%] 600°C
pristine	294±5	363±1	341±0	86±3
VI/Cu	294±3	364±2	339±1	84±1

Fig. 8 Results of TG/DTG analysis of pristine and Cu modified viscose nonwoven fabrics

Bioactivity

Cu sputtered nonwoven fabrics is characterized by strong antibacterial activity (A ≥ 3) (Table 3). Relatively weaker impact activity is observed in the case of Gram-positive bacteria *Staphylococcus aureus*. Gram-negative bacteria *Klebsiella pneumoniae* has a thin peptidoglycan layer and an outer lipid membrane. In Gram-positive bacteria the peptidoglycan layer is significantly thicker and an outer lipid membrane is not present (San et al. 2015). Similar results were reported by Vaidya and co-authors who studied antibacterial activity of copper against Gram-negative bacteria *Klebsiella pneumoniae* and *Acinetobacter baumanni* and Gram-positive *Enterococcus faecium* (Vaidya et al. 2017).

In our previous work, we found that PET/Cu and CO/Cu woven fabrics, sputtered with Cu in the same way showed both not only antibacterial properties but also antiviral activity (Cieślak et al. 2022). CO/Cu fabric has good antiviral activity in relation to vaccinia virus (VACV), herpes simplex virus type 1 (HSV-1) and influenza A virus H1N1 (IFV) and weak activity against mouse coronavirus (MHV). PET/Cu fabric has weak antiviral activity against HSV-1 and MHV. The mean values of Cu content determined by the AAS method were 15.2 g/kg and 12.6 g/kg for PET/Cu and CO/Cu fabrics, respectively. The antiviral properties for Cu modified viscose nonwoven fabric studies in this report showed different results. Cu content (AAS) for Cu modified viscose nonwoven is 22.2 g/kg. However, Cu modified viscose nonwoven fabric characterized by higher content of Cu revealed lower antiviral activity. The Cu modified viscose nonwoven showed weak antiviral activity only against HSV-1 (Table 5), because according to the standard 18,184:2019, *Textiles-Determination of antiviral activity of textile products*, good antiviral activity is described as 3.0 > Mv ≥ 2.0 (Table 4).

Taking into account the possibility of using a modified viscose nonwoven as a material which has direct contact with the skin, cytotoxicity is an important parameter to assess the material safety. Figure 9 shows the values of cell viability determined for both pristine and Cu modified viscose nonwovens. The results indicate that modified nonwoven has no significant toxicity compared to both the control medium and pristine nonwoven fabric ($p \geq 0.05$).

These bioactive results indicate that the Cu content is not a determining factor in the effectiveness of antiviral activity. The crucial issue is also the type of modified textile structure. Cu coating has a different thickness and in some longitudinal grooves, characteristic for viscose fibers, (especially with greater depth) the surface is not covered with copper (Fig. 3). Effect of Cu deposition depends also on the position

Table 4 The antiviral activity values of M_v (log reduction V_c/V_t) of Cu modified nonwoven fabric against VACV, HSV-1, IFV and MHV viruses. The control sample was pristine nonwoven

Sample	Mv, Log reduction			
	PFU/ml VACV	PFU/ml HSV-1	TCID50/ml IFV	TCID50/ml MHV
VI/Cu	0	1	0	0

Table 3 Antibacterial activity of Cu modified nonwoven fabric

	Staphylococcus aureus (ATCC 6538)	*Klebsiella pneumoniae* (ATCC 4352)
Concentration of inoculum, CFU/ml	2.0×10^5	2.0×10^5
*Growth value F—*for the control sample* (pristine) $F = \lg C_t - \lg C_o$	1.70 $\lg C_t$: − 4.48 $\lg C_o$: − 6.18	1.74 $\lg C_t$: − 4.88 $\lg C_o$: − 6.62
*Growth value G—*for the test sample* (Cu modified) $G = \lg T_t - \lg T_o$	0.64 $\lg T_t$: − 1.94 $\lg T_o$: < 1.30	0.30 $\lg T_t$: − 1.60 $\lg T_o$: < 1.30
*Value of antimicrobial activity A A = F − G	4.24	5.02
Time and temperature of incubation	22 h + 48 h (37 ± 2 °C)	

*Calculation method according to PN-EN ISO 20743 Determination of antimicrobial activity of finished products with antibacterial finish. Assessment of antimicrobial activity according to EN ISO 20743:2013, app. F, where: 2 ≤ A < 3 significant, A ≥ 3 strong

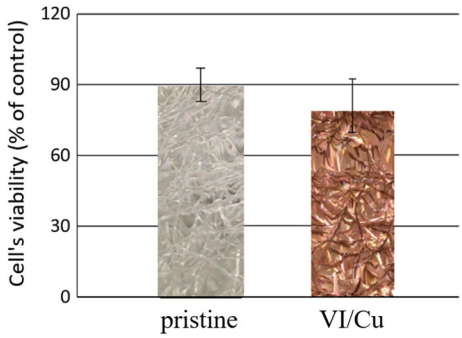

Fig. 9 Toxicity of tested nonwoven fabric based on MTT test

of the fibers in the structure of the nonwoven fabric in their sputtered top layer. Moreover, only one side of the nonwoven fabric was modified which may affect the antiviral properties. The efficiency of the sputtering process of nonwoven textile structures, characterized by spatial 3D structure, and surface availability to Cu atoms play crucial roles in the antiviral properties of the modified samples. Therefore, bioactive functionalization should take into account both the properties of the modifier and the modified material, including fibers surface morphology and fabric structure. During the pandemic, many studies were conducted on the activity of metallic coatings against microorganisms, most often applied to flat surfaces (resins, glass, Si wafers, etc.) (Hsu and Wu 2019; Bhattacharjee et al. 2021). Moreover, in the case of textiles used for protection against microorganisms (e.g. masks, filters, clothing), a bioactive effectiveness, safety and comfort of use should be reached. The issue of optimally designing fabrics used as anti-epidemic protection against SARS have been well documented (Kwong et al. 2021). Compaction and sealing of material structures used to protection of the respiratory system caused the increase in airflow resistance and, as a result, discomfort and health problems (Bhattacharjee et al. 2021).

Wettability and surface free energy

After modification the surface properties of Cu sputtered surface of the nonwoven fabric were changed. The values of the contact angle (Table 5) increased for water and formamide. The value of the surface free energy γ_S determined on the basis of the contact angles is lower for the modified nonwoven fabric by 23.9%, which is mainly due to the decrease in the value of the dispersion component γ_S^d by 26.7%. The value of the polar component γ_S^p increased 30-fold, but still is very low of 0.60 mJ/m^2. Examplary images of water droplets on the pristine and Cu sputtered surface of the fabric are shown in Fig. 10.

The apparent contact angle is defined as the angle between the apparent solid surface and the tangent to the liquid-fluid interface. For two-dimensional systems there exists a correspondence between this theory and measured contact angles. Research on the wettability phenomenon has been going on for many years and new models or improvements to existing ones are proposed. Wenzel was the first to discuss the influence of roughness on apparent contact angle (Wenzel 1936). However, a more complex model was needed for heterogeneous systems, which was proposed by Cassie and Baxter (the Cassie–Baxter equation) (Cassie and Baxter 1944). The wetting of textiles even made of the same polymer is determined by the surface topography, geometry of the elementary fiber and fabric structures. In the case of diversified and spatial nonwoven structures, this issue is

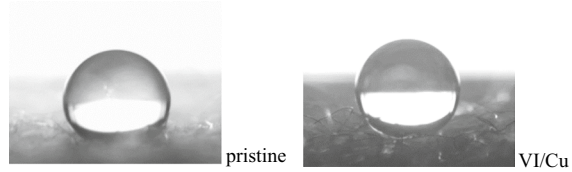

Fig. 10 Exemplary images of water droples on pristine and Cu modified surface of nonwovens fabric

Table 5 The values of the contact angle and the surface free energy

Sample	Contact angle Θ, deg			Surface free energy with dispersive and polar components, γmJ/m^2		
	Θ_W	Θ_F	Θ_H	γ_S	γ_S^d	γ_S^p
Pristine	118.2	87.3	0.0	20.50	20.48	0.02
VI/Cu	127.6	116.5	0.0	15.61	15.01	0.60

complex. Using of the single fiber prepared from nonwoven fabric and Wilhelmy test may be an appropriate method to assess fiber wettability, but the results will be valid for fibers, not for nonwoven fabrics, likewise in the case of the Washburn methods (Cieślak et al. 2012; Bahners and Gutmann 2020). On the other hand, determining the contact angles by the sessile drop method can be useful for comparative measurements of samples to characterize the effects of surface modification (Cieślak et al. 2012; Eid et al. 2018; Peng et al. 2018; Kowalski et al. 2022). Viscose is generally characterized by hydrophilic properties. In the case of unmodified viscose needle-punched nonwoven fabric the water contact angle is of 118°, so the nonwoven surface is hydrophobic. This is due to the fact that the surface topography has a significant impact on the value of the wetting angle. On solid, homogeneous smooth surfaces, the component of interactions with air is neglected and the solid–liquid interactions dominate. In the case of this nonwoven fabric (Fig. 1), there are significantly large air-filled areas on the surface, and the solid–liquid contact area is limited. A porous surface is a heterogeneous surface formed by a solid and air. According to Cassie and Baxter (Cassie and Baxter 1944), the cosine of the contact angle of a heterogeneous surface corresponds to the sum of the cosines of the contact angle of two homogeneous surfaces—solid and air, depending on their mutual ratio. The Cassie and Baxter equation has the form:

$$\cos\Theta' = -1 + \varphi_s(1 + \cos\Theta)$$

where φ_s is a fraction of the solid in contact with the liquid. In the case of high porosity/roughness of the surface, the value of fraction φ_s tends to zero, and Θ' tends to 180°.

Electrical properties

Although electret filters are used to air filtration and purification, antistatic properties are expected in the case of materials intended for personal masks or clothing. The material susceptible to the accumulation of static charge causes the deposition of contaminated dust particles and impairs the airflow and comfort of use. The values of half decay time (t_{50}) of nonwoven fabrics modified with Cu are lower than 0.01 s and shielding factors (S) are above 0.95 (Table 6). According to standard PN-EN 1149-5:2018 Cu modified viscose nonwoven fabrics can be classified as an electrostatic dissipative because $t_{50} < 4$ s and additionally $S > 0.2$. Moreover, the surface resistance after the modification takes values of order 10^3 Ω (Table 6), thus the nonwoven also meets the second alternative criterion of this standard—*or the surface resistance is* $\leq 2.5 \times 10^9$ *Ω on at least one surface or the surface resistance* $\leq 2.5 \times 10^9$ *Ω on one surface at least*. The volume resistance after the modification decreased by two or three orders of magnitude, respectively for relative humidity of 25% and 50% as a result of susceptibility of viscose fibers to water sorption.

Comfort parameters

The comfort properties are essential for further application in various protective textile products, such as masks and clothes. The key parameters are air permeability and water vapor permeability.

Table 6 Results of resistance and charge decay of pristine and Cu modified fabric

Sample	Resistance		Charge decay—induction method	
	Surface $\mathbf{R_S}$, Ω	Volume $\mathbf{R_V}$, Ω	Half decay time $\mathbf{t_{50}}$, s	Shielding factor **S**
RH = 25 ± 5%; temp. 23 ± 2 °C				
Pristine	$1.66 \times 10^{10} \pm 0.11 \times 10^{10}$	$7.80 \times 10^9 \pm 0.47 \times 10^9$	0.27 ± 0.17	0.0
VI/Cu	$0{,}73 \times 10^3 \pm 0.13 \times 10^3$	$6.28 \times 10^7 \pm 0.79 \times 10^7$	< 0.01	0.95 ± 0,07
RH = 50 ± 2%; temp. 23 ± 1 °C				
Pristine	$3.17 \times 10^9 \pm 0.10 \times 10^9$	$1.11 \times 10^9 \pm 0.16 \times 10^9$	0.07 ± 0.01	0.0
VI/Cu	$0.54 \times 10^3 \pm 0.08 \times 10^3$	$9.80 \times 10^6 \pm 0.68 \times 10^6$	< 0.01	0.97 ± 0.01

Both parameters for viscose nonwoven fabric indicate the sufficient comfort properties for protective textile materials. After the modification the values of these parameters were not deteriorated. The air permeability decreased slightly (about 8%) (Fig. 11), as result of the slight changes in the layer structure sputtered by Cu. The water vapor permeability remained at the same level (Fig. 11).

Breathing resistance measurement

The tests of breathing resistance were carried out to assess the possibility of using a modified viscose nonwoven fabric as a filtering element for respiratory protection devices (e.g. filtering half-masks). Table 7 shows a model of a face mask made of modified viscose nonwoven fabric with a filtration area of approx. 150 cm^2 and obtained results of breathing resistance test. It was found that the magnetron sputtering of the viscose nonwoven with copper did not affect its breathing resistance when the inhalation flow rate

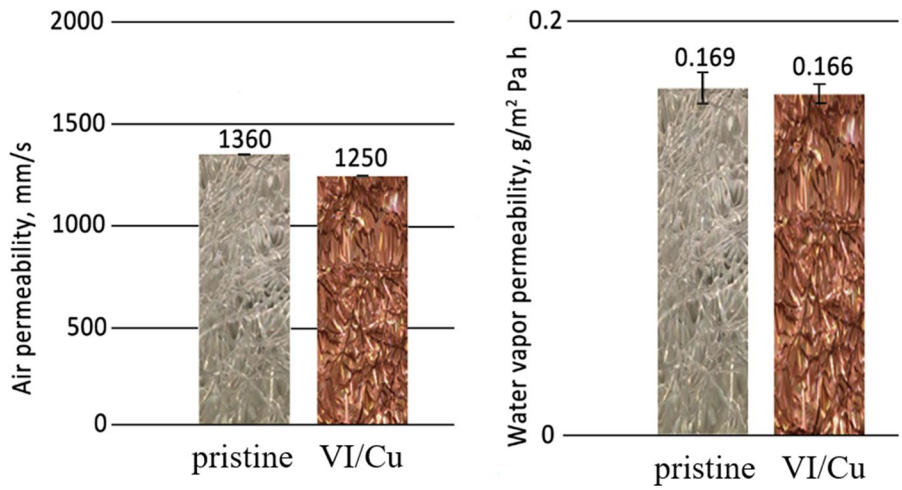

Fig. 11 The values of the air permeability and the water vapor permeability for pristine and Cu modified nonwoven

Table 7 Results of inhalation and exhalation airflow resistance of masks made of pristine and Cu modified viscose nonwoven fabrics. The image of the Mask and respirator breathing resistance tester (inset)

	Sample	Inhalation resistance, Pa		Exhalation resistance, Pa
		within 30 L/min	within 95 L/min	within 160 L/min
	Pristine	6.7 ± 0.2	28.5 ± 1.1	43.9 ± 1.2
	VI/Cu	5.2 ± 0.5	28.7 ± 0.9	50.3 ± 1.1

was 30 and 95 L/min. In the breathing resistance on exhalation with the air flow of 160 L/min the 14% increase was observed.

The values of the maximum permissible breathing resistance (at a specific air flow) for a filter element used in respiratory protective devices are specified in the international standards EN 149-2001 + A1:2009. *Respiratory protective devices—Filtering half masks to protect against particles—Requirements, testing, marking*, GB 2626-2019 *Respiratory protection—Non-powered air-purifying particle respirator*, NIOSH 42 CFR Part 84-2019. *Respiratory Protective Devices*. Nonwovens were measured in accordance with the EN 149-2001 + A1:2009 standard, in which the maximum permissible resistance inhalation within the air flow of 30 and 95 L/min, depending on the protection classes, is in the range of 60–100 and 210–300 Pa, respectively. However, the maximum permissible resistance exhalation at a flow rate of 160 L/min is 300 Pa.

Taking into account the above criteria and the obtained results, it can be concluded that both pristine and Cu modified viscose nonwoven meet the requirements of breathing resistance for all protection classes (FFP1, FFP2 and FFP3) specified in the EN 149-2001 standard. It should be noted that the breathing resistance depends not only on the properties of the filtering element, but also on the type of mask (e.g. flat, folded, cup-shaped, 3D printed), and thus on its proper fit and adherence to the face (Ramos et al. 2022; Wang et al. 2022).

Conclusions

In this study, magnetron sputtering method is applied for the first time to modify of the spatial 3-D viscose needle-punched nonwoven fabric with copper. Cu modified nonwoven is characterized by antimicrobial activity, hydrophobic properties and high electrical conductivity, good air and water vapor permeability, and meets the requirements of breathing resistance for all protection classes (FFP1, FFP2 and FFP3) specified in the EN 149-2001 standard. It also has no significant toxicity compared to the control medium and pristine nonwoven fabric. The current state of knowledge regarding the efficacy of Cu-based nanoparticles and materials functionalized with them shows this way promising direction in the development of antibacterial and antiviral surface coating. Our research has shown that the spatial nonwoven structure made of regenerated cellulose fibers and one-side sputtered with copper by magnetron technique has an antibacterial effect against Gram-positive *Staphylococcus aureus* (ATCC 6538) and Gram-negative *Klebsiella pneumoniae* (ATCC 4352), but slightly weaker compared to a flat cotton fabric with almost two-fold lower copper content. In the case of herpes simplex virus type 1 (HSV-1) McKrae strain, vaccinia virus (VACV) WR strain (ATCC VR-1736), influenza A virus H1N1 (IFV) (ATCC VR-1736) and mouse coronavirus (MHV) JHV strain (ATCC VR-765) used in the study, Cu modified nonwoven fabric has weak activity against herpes simplex virus type 1 (HSV-1). The antiviral effect depends not only on the copper content, but also on the structure of textile material. Our research so far has shown that different textiles materials modified in the same way show different activity against the same viruses. Effect of Cu sputtering depends *inter alia* on the position of the fibers in the spatial 3-D structure of the nonwoven and their aligment to sputtering target. The flat textile materials with high density structure allow the formation an uniform layer of copper, but if the structure is too thight, such modification may increase their airflow resistance. In turn, a loose, disordered spatial structure ensures good air and water vapor transport, but in the case of sputtering or spraying methods, the bioactive modifier may be applied unevenly. The design of textile protective materials with antimicrobial properties should therefore take into account mentioned aspects, which will be the subject of our further research.

Acknowledgments The research was carried out within the National Centre for Research and Development project number DOB-SZAFIR/02/B/004/02/2021 using the apparatus purchased in projects: POIG.01.03.01-00-004/08 Functional nano- and micro textile materials—NANOMITEX cofinanced by the European Regional Development Fund and the National Centre for Research and Development and WND-RPLD.03.01.00-001/09, cofinanced by the European Regional Development Fund and the Ministry of Culture and National Heritage. The authors would like to thank Arkadiusz Szwugier, Alicja Nejman, Maciej Piórkowski and Stanisława Wróbel for their excellent technical contributions.

Author contributions This manuscript was written thanks to contributions of all authors. The first draft of the manuscript was written by MC and all authors commented on previous versions of the manuscript.

Funding This work have been granted by the National Centre for Research and Development—project DOB-SZAFIR/02/B/004/02/2021.

Data availability Data is available on request from the corresponding author on reasonable request.

Declarations

Conflict of interest The authors have no relevant financial or non-financial interests to disclose.

Ethical approval Not applicable.

Consent to participate Not applicable.

Consent for publication All the authors agreed with the publication of the present manuscript in Cellulose.

References

Ali A, Baheti V, Militky J et al (2018) Copper coated multifunctional cotton fabrics. J Ind Text 48:448–464. https://doi.org/10.1177/1528083717732076

Anu A, Abdul Khadar M (2015) Grain size tuning of nanostructured Cu_2O films through vapour phase supersaturation control and their characterization for practical applications. AIP Adv. https://doi.org/10.1063/1.4932087

Bahners T, Gutmann JS (2020) Procedures for the characterization of wettability and surface free energy of textiles—use, abuse, misuse and proper use: a critical review. In: Mittal KL (ed) Progress in adhesion and adhesives. Wiley, pp 259–293

Balasubramaniam B, Prateek RS et al (2021) Antibacterial and antiviral functional materials: chemistry and biological activity toward tackling COVID-19-like pandemics. ACS Pharmacol Transl Sci 4:8–54. https://doi.org/10.1021/acsptsci.0c00174

Barreca D, Gasparotto A, Tondello E (2007) CVD Cu_2O and CuO nanosystems characterized by XPS. Surf Sci Spectra 14:41–51. https://doi.org/10.1116/11.20080701

Bell T (2020) The ancient history of copper. https://www.thoughtco.com/copper-history-pt-i-2340112

Bhattacharjee S, Bahl P, De Silva C et al (2021) Experimental evidence for the optimal design of a high-performing cloth mask. ACS Biomater Sci Eng 7:2791–2802. https://doi.org/10.1021/acsbiomaterials.1c00368

Biesinger MC (2017) Advanced analysis of copper X-ray photoelectron spectra. Surf Interface Anal 49:1325–1334. https://doi.org/10.1002/sia.6239

Borkow G (2012) Using copper to fight microorganisms. Curr Chem Biol 6:93–103. https://doi.org/10.2174/187231312801254723

Borkow G, Zhou SS, Page T, Gabbay J (2010) A novel anti-influenza copper oxide containing respiratory face mask. PLoS One. https://doi.org/10.1371/journal.pone.0011295

Bula K, Koprowska J, Janukiewicz J (2006) Application of cathode sputtering for obtaining ultra-thin metallic coatings on textile products. Fibres Text East Eur 14:75–79

Carrillo F, Colom X, Suñol JJ, Saurina J (2004) Structural FTIR analysis and thermal characterisation of lyocell and viscose-type fibres. Eur Polym J 40:2229–2234. https://doi.org/10.1016/j.eurpolymj.2004.05.003

Cassie ABD, Baxter S (1944) Wetting of porous surfaces. Trans Faraday Soc 40:546–551

Champagne V, Sundberg K, Helfritch D (2019) Kinetically deposited copper antimicrobial surfaces. Coatings 9:1–9. https://doi.org/10.3390/coatings9040223

Cieślak M, Puchowicz D, Schmidt H (2012) Evaluation of the possibility of using surface free energy study to design protective fabrics. Text Res J 82:1177–1189. https://doi.org/10.1177/0040517511426612

Cieślak M, Kowalczyk D, Krzyżowska M et al (2022) Effect of Cu modified textile structures on antibacterial and antiviral protection. Materials 15:1–16. https://doi.org/10.3390/ma15176164

da Ramos CMC, dos Santos JRL, Teixeira RB (2022) Development of mask design as personal protective equipment through 3D printing. Mater Today Proc 70:168–178

Dobromir M, Biliuta G, Luca D et al (2011) XPS study of the ion-exchange capacity of the native and surface oxidized viscose fibers. Colloids Surfaces A Physicochem Eng Asp 381:106–110. https://doi.org/10.1016/j.colsurfa.2011.03.030

Eid KF, Panth M, Sommers AD (2018) The physics of water droplets on surfaces: exploring the effects of roughness and surface chemistry. Eur J Phys. https://doi.org/10.1088/1361-6404/aa9cba

Giesz P, Celichowski G, Puchowicz D et al (2016) Microwave-assisted TiO_2: anatase formation on cotton and viscose fabric surfaces. Cellulose 23:2143–2159. https://doi.org/10.1007/s10570-016-0916-z

Grass G, Rensing C, Solioz M (2011) Metallic copper as an antimicrobial surface. Appl Environ Microbiol 77:1541–1547. https://doi.org/10.1128/AEM.02766-10

Gurianov Y, Nakonechny F, Albo Y, Nisnevitch M (2019) Antibacterial composites of cuprous oxide nanoparticles and polyethylene. Int J Mol Sci 20:439. https://doi.org/10.3390/ijms20020439

Han J, Zong X, Zhou X, Li C (2015) Cu2O/CuO photocathode with improved stability for photoelectrochemical

water reduction. RSC Adv 5:10790–10794. https://doi.org/10.1039/c4ra13896a

Hans M, Erbe A, Mathews S et al (2013) Role of copper oxides in contact killing of bacteria. Langmuir 29:16160–16166. https://doi.org/10.1021/la404091z

Hashmi M, Ullah S, Kim IS (2019) Copper oxide (CuO) loaded polyacrylonitrile (PAN) nanofiber membranes for antimicrobial breath mask applications. Curr Res Biotechnol 1:1–10. https://doi.org/10.1016/j.crbiot.2019.07.001

Hiraba H, Koizumi H, Kodaira A et al (2021) Effects of copper surface oxidation and reduction on shear-bond strength using functional monomers. Materials 14:1–11. https://doi.org/10.3390/ma14071753

Hsu YH, Wu WY (2019) Antibacterial Ag-Cu coatings deposited using an asymmetric bipolar high-power impulse magnetron sputtering technique. Surf Coatings Technol 362:302–310. https://doi.org/10.1016/j.surfcoat.2019.02.001

Huang ML, Lu SG, Zhou JJ et al (2022) Metallic coloration with Cu/CuO coating on polypropylene nonwoven fabric via a physical vapor deposition method and its multifunctional properties. J Text Inst 113:1345–1354. https://doi.org/10.1080/00405000.2021.1928995

Hussain FS, Abro NQ, Ahmed N et al (2022) Nano-antivirals: a comprehensive review. Front Nanotechnol 4:1–27. https://doi.org/10.3389/fnano.2022.1064615

Imani SM, Ladouceur L, Marshall T et al (2020) Antimicrobial nanomaterials and coatings: current mechanisms and future perspectives to control the spread of viruses including SARS-CoV-2. ACS Nano 14:12341–12369. https://doi.org/10.1021/acsnano.0c05937

Jiang P, Prendergast D, Borondics F et al (2013) Experimental and theoretical investigation of the electronic structure of Cu_2O and CuO thin films on Cu(110) using x-ray photoelectron and absorption spectroscopy. J Chem Phys 138:024704. https://doi.org/10.1063/1.4773583

Jrajri K, Beraich M, Warad I et al (2022) Electrodeposition of Cu2O thin film onto copper substrate by linear sweep voltammetry at low duration: Effect of bath pH. Biointerface Res Appl Chem. 12:7715–7724. https://doi.org/10.33263/BRIAC126.77157724

Jung S, Byeon EY, Kim DG et al (2021) Copper-coated polypropylene filter face mask with SARS-CoV-2 antiviral ability. Polymers (basel) 13:1–10. https://doi.org/10.3390/polym13091367

Jung S, Yang JY, Jang D et al (2022) Sustainable antibacterial and antiviral high-performance copper-coated filter produced via ion beam treatment. Polymers 14:1007. https://doi.org/10.3390/polym14051007

Kärber G (1931) Beitrag zur kollektiven Behandlung pharmakologischer. Beitrag zur Kollekt Behandlung pharmakologischer Reihenversuche 1–4

Kelly PJ, Arnell RD (2000) Magnetron sputtering: A review of recent developments and applications. Vacuum 56:159–172. https://doi.org/10.1016/S0042-207X(99)00189-X

Kharaghani D, Khan MQ, Tamada Y et al (2018) Fabrication of electrospun antibacterial PVA/Cs nanofibers loaded with CuNPs and AgNPs by an in-situ method. Polym Test 72:315–321. https://doi.org/10.1016/j.polymertesting.2018.10.029

Koprowska J, Dobruchowska E, Reszka K, Szwugier A (2015) Morphology and electromagnetic shielding effectiveness of PP nonwovens modified with metallic layers. Fibres Text East Eur 23:84–91. https://doi.org/10.5604/12303666.1161763

Kowalski M, Salerno-Kochan R, Kamińska I, Cieślak M (2022) Quality and quantity assessment of the water repellent properties of functional clothing materials after washing. Materials. https://doi.org/10.3390/ma15113825

Kudzin M, Mrozinska Z, Kaczmarek A, Lisiak-Kucinska A (2020) Deposition of Copper on Poly (Lactide) Non-Woven Fabrics by Magnetron Sputtering—Fabrication of. Materials (basel) 13:1–16

Kwong LH, Wilson R, Kumar S et al (2021) Review of the breathability and filtration efficiency of common household materials for face masks. ACS Nano 15:5904–5924. https://doi.org/10.1021/acsnano.0c10146

Li C, Yamahara H, Lee Y et al (2015) CuO nanowire/microflower/nanowire modified Cu electrode with enhanced electrochemical performance for non-enzymatic glucose sensing. Nanotechnology. https://doi.org/10.1088/0957-4484/26/30/305503

Lin N, Verma D, Saini N et al (2021) Antiviral nanoparticles for sanitizing surfaces: A roadmap to self-sterilizing against COVID-19. Nano Today 40:101267. https://doi.org/10.1016/j.nantod.2021.101267

Liu Z, Ye J, Rauf A et al (2021) A flexible fibrous membrane based on copper(ii) metal-organic framework/poly(lactic acid) composites with superior antibacterial performance. Biomater Sci 9:3851–3859. https://doi.org/10.1039/d1bm00164g

Marković D, Vasiljević J, Ašanin J et al (2020) The influence of coating with aminopropyl triethoxysilane and CuO/Cu_2O nanoparticles on antimicrobial activity of cotton fabrics under dark conditions. J Appl Polym Sci 137:1–12. https://doi.org/10.1002/app.49194

Markowska-Szczupak A, Paszkiewicz O, Michalkiewicz B et al (2021) Fabrication of antibacterial metal surfaces using magnetron-sputtering method. Materials 14:7301. https://doi.org/10.3390/ma14237301

Meister TL, Fortmann J, Breisch M et al (2022) Nanoscale copper and silver thin film systems display differences in antiviral and antibacterial properties. Sci Rep 12:1–10. https://doi.org/10.1038/s41598-022-11212-w

Miura TA, Travanty EA, Oko L et al (2008) The spike glycoprotein of murine coronavirus MHV-JHM mediates receptor-independent infection and spread in the central nervous systems of ceacam1a −/− mice. J Virol 82:755–763. https://doi.org/10.1128/jvi.01851-07

Nowak I, Krucińska I, Januszkiewicz Ł (2019) Metallic electroconductive transmission lines obtained on textile substrates by magnetron sputtering. Fibres Text East Eur 27:51–57. https://doi.org/10.5604/01.3001.0013.0742

Owens DK, Wendt RC (1969) Estimation of the surface free energy of polymers. J Appl Polym Sci 13:1741–1747. https://doi.org/10.1002/app.1969.070130815

Peng L, Guo R, Lan J et al (2018) Preparation and characterization of copper-coated polyester fabric pretreated with laser by magnetron sputtering. J Ind Text 48:482–493. https://doi.org/10.1177/1528083717736101

Poulston S, Parlett PM, Stone P, Bowker M (1996) Surface oxidation and reduction of CuO and Cu_2O studied using XPS and XAES. Surf Interface Anal 24:811–820. https://doi.org/10.1002/(SICI)1096-9918(199611)24:12%3c811::AID-SIA191%3e3.0.CO;2-Z

San K, Long J, Michels CA, Gadura N (2015) Antimicrobial copper alloy surfaces are effective against vegetative but not sporulated cells of gram-positive Bacillus subtilis. Microbiologyopen 4:753–763. https://doi.org/10.1002/mbo3.276

Sharma V, Basak S, Ali SW (2022) Synthesis of copper nanoparticles on cellulosic fabrics and evaluation of their multifunctional performances. Cellulose 29:7973–7988. https://doi.org/10.1007/s10570-022-04709-0

Sülar V, Devrim G (2019) Biodegradation behaviour of different textile fibres: visual, morphological, structural properties and soil analyses. Fibres Text East Eur 27:100–111. https://doi.org/10.5604/01.3001.0012.7751

Szymańska E, Orłowski P, Winnicka K et al (2018) Multifunctional tannic acid/silver nanoparticle-based mucoadhesive hydrogel for improved local treatment of HSV infection: in vitro and in vivo studies. Int J Mol Sci 19:387. https://doi.org/10.3390/ijms19020387

Vaidya MY, McBain AJ, Butler JA et al (2017) Antimicrobial efficacy and synergy of metal ions against enterococcus faecium, klebsiella pneumoniae and acinetobacter baumannii in planktonic and biofilm phenotypes. Sci Rep 7:1–9. https://doi.org/10.1038/s41598-017-05976-9

Vesel A, Mozetic M, Strnad S et al (2009) Plasma modification of viscose textile. Vacuum 84:79–82. https://doi.org/10.1016/j.vacuum.2009.04.028

Vihodceva S, Kukle S, Blums J, Zommere G (2011) The effect of the amount of deposited copper on textile surface light reflection intensity. Technology 6:24–29

Wang W, Chen T, Li Z et al (2022) Comparison of filtration efficiency and respiratory resistance of COVID-19 protective masks by multi-national standards. Am J Infect Control 50:516–524. https://doi.org/10.1016/j.ajic.2022.02.009

Was-Gubala J, Machnowski W (2014) Application of Raman spectroscopy for differentiation among cotton and viscose fibers dyed with several dye classes. Spectrosc Lett 47:527–535. https://doi.org/10.1080/00387010.2013.820760

Wenzel RN (1936) Resistance of solid surfaces to wetting by water. Ind Eng Chem 28:988–994. https://doi.org/10.1021/ie50320a024

Wiśniewski B, Koprowska J (2014) Textile barrier materials protecting against electromagnetic field (EMF) radiation obtained by magnetron sputtering method. Przegląd Włókienniczy Włókno, Odzież, Skóra 2:29–32

Yamamoto S, Bluhm H, Andersson K et al (2008) In situ x-ray photoelectron spectroscopy studies of water on metals and oxides at ambient conditions. J Phys Condens Matter 20:184025. https://doi.org/10.1088/0953-8984/20/18/184025

Zhang S, Dong H, He R et al (2022) Hydro electroactive Cu/Zn coated cotton fiber nonwovens for antibacterial and antiviral applications. Int J Biol Macromol 207:100–109. https://doi.org/10.1016/j.ijbiomac.2022.02.155

Ziaja J, Koprowska J, Janukiewicz J (2008) Using plasma metallisation for manufacture of textile screens against electromagnetic fields. Fibres Text East Eur 16:64–66